Measurement-Based Multiple-Scattering Model of Small-Scale Fading in High-Speed Railway Cutting Scenarios

Zhang, Bei; Zhong, Zhangdui; He, Ruisi; Tufvesson, Fredrik; Ai, Bo

Published in:
IEEE Antennas and Wireless Propagation Letters

DOI:
10.1109/LAWP.2016.2626303

2017

Document Version:
Peer reviewed version (aka post-print)

Measurement-Based Multiple-Scattering Model of Small-Scale Fading in High-Speed Railway Cutting Scenarios

Bei Zhang, *Student Member, IEEE,* Zhangdui Zhong, *Senior Member, IEEE,* Ruisi He, *Member, IEEE,* Fredrik Tufvesson, *Senior Member, IEEE,* and Bo Ai, *Senior Member, IEEE*

***Abstract*—In this paper, the fading statistics of wireless channels in high-speed railway cutting scenarios are characterized based on measurements. A multiple scattering model called second-order scattering fading (SOSF) is used to model the small-scale fading considering the influence of cuttings and bridges. The SOSF model can offer the possibility of analytical estimation for different fading severities via a simple moment-based estimator. It is demonstrated that Ricean fading is the dominant fading distribution in cutting scenarios but deep fades also occur. The fading process is therefore described by a hidden Markov model, which is validated statistically by measurement data.**

***Index Terms*—High speed railway, cutting, small-scale fading, multiple scattering channel model.**

I. Introduction

TO enable reliable communication in high speed railway (HSR) wireless networks, a thorough understanding of the channel behavior is vital. Channel fading is usually divided into large-scale fading (LSF) and small-scale fading (SSF). SSF refers to the changes in signal amplitude and phase over areas in the order of a wavelength due to constructive and destructive summation of multi-path components. The characteristics of the SSF have a strong influence on the selection of radio transmission technologies such as diversity schemes and equalization methods. Various statistical distributions, including Rayleigh, Rice, Nakagami-*m* and Weibull, are used to describe the SSF in multipath propagation channels. While the Ricean distribution can be used to represent line-of-sight (LOS) fading conditions of differing severity, the parametrization of the fading severity parameter is less flexible. Moreover, empirical and theoretical studies have shown that the commonly used Nakagami-*m* fading model cannot represent LOS wireless channels well [1] [2]. In terrain cutting (also called U-shape cutting) scenarios, the SSF behavior is also different from the classical fading distributions given the particular layout and the occasional presence of blocking objects such as bridges. Recently, some geometry-based models are proposed for the cutting scenario [3] [4]. In [5] the authors analyzed the SSF characteristics including multipath number, delay spread, and Doppler spread on the basis of wideband HSR channel measurements. However, little work on the SSF modeling of cuttings has been undertaken.

In our previous work [6-8], the SSF characteristics, including fading depth, level crossing rate, average fade duration and Ricean K-factor were studied. It was shown that based on an Akaike's information criterion evaluation, the Ricean distribution can be used to describe the SSF in HSR cutting scenarios. In this letter, we make a detailed investigation of the SSF by using a multi-scattering model to analyze occasional changes in the fading statistics.

TABLE I
Measurement Parameters.

Parameter	Value
Center frequency	930 MHz
Bandwidth	200 kHz
Tx antenna height (to cutting top)	28 m
Rx antenna height (including train)	4.1 m
Tx power at antenna output	43 dBm
Sampling interval	10 cm
Average Rx speed	270 km/h
Directivity of Tx/Rx antenna	Directional/omnidirectional

II. Measurement Description

Narrowband measurements are performed along the "Zhengzhou-Xi'an" HSR line in China. Real base stations are used as transmitters (Tx), usually positioned 15 m to the side of the cutting. The receiver (Rx) is composed of a Willtek 8300 Griffin fast measurement receiver, a distance sensor, and GPS receiver. A more detailed description of the measurement system can be found in [7]. A summary of the measurement parameters is given in Table I.

A terrain cutting is a semi-enclosed construction usually with two slopes along the track, and constitutes a common scenario in HSR environments. Usually, the slope is composed of concrete and stone with some grass covering the surface. In addition, there are typically scatters such as pillars holding the power lines along the track. It is noteworthy that bridges, that cross the railway, are common in order to enable necessary transportation on both side of terrain cuttings. The cross-bridges lead to occasional non-line-of-sight (NLOS) propagation. As a result, there is in general clear

This work is supported by the National Natural Science Foundation of China (61501020, 61222105, 61471030, U1334202), the Fundamental Research Funds for the Central Universities (2016JBZ006, 2016YJS012, 2016JBM075), State Key Lab of Rail Traffic Control and Safety Project (RCS2016ZT021), and China Postdoctoral Science Foundation (2016M591355).
(*Corresponding author: Ruisi He.*) B. Zhang, Z. Zhong, R. He and B. Ai are with the State Key Laboratory of Rail Traffic Control and Safety, Beijing Jiaotong University, Beijing 100044, China (e-mail: zbandysun@gmail.com; zhdzhong@bjtu.edu.cn; ruisi.he@ieee.org; boai@bjtu.edu.cn). F. Tufvesson is with the Department of Electrical and Information Technology, Lund University, 221 00 Lund, Sweden (e-mail: fredrik.tufvesson@eit.lth.se).

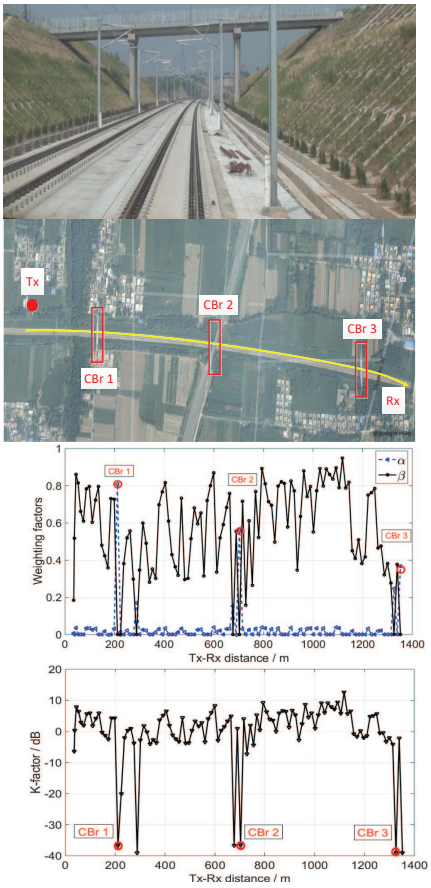

Fig. 1. Estimated results in Cutting 1: Cutting scenario with a crossing bridge, aerial view, weighting factors, and Ricean K-factor versus distance. Red circles indicate the positions of cross bridges.

LOS in the cutting scenario. However, the effects of reflected and scattered components can sometimes be strong due to occasional blocking.

In order to investigate the SSF statistics, six cuttings along the HSR track are taken and the measurements are conducted four times in cutting 1, 2 and three times for the rest of them. Two kinds of cutting environments, including suburban (No. 1-3, buildings are typically low residential or townhouses with one or few floors) and rural (No. 4-6, a predominantly open area), are used for the analysis. Detailed structural parameters of the cuttings are given in [7].

III. Second-order Scattering Fading Distribution

Overlapping windows with an interval of ten wavelengths and a window size of twenty wavelengths, are used to provide the mean signal level for the evaluation of the SSF. The sampling interval (10 cm) is less than half the wavelength and we have 222300 samples in total. This gives us sufficient statistics for the analysis of the SSF distribution.

In order to analyze the SSF, we model the channel as a sum of multiple scattering components. In peer-to-peer communication systems, the time-variant SSF can in some cases be described by a second-order scattering fading (SOSF) model as proposed in [9] [10] as

$$S_{SOSF}(t) = w_0 e^{j\theta} + w_1 G_1(t) + w_2 G_2(t) G_3(t), \qquad (1)$$

where $w_0 e^{j\theta}$ is the LOS component with weighting factor w_0 and θ is an uniformly distributed phase in $[0, 2\pi]$. G_i are independent identically distributed (i.i.d.) complex Gaussian random variables with zero mean and unit variance. Moreover, the weighting factors $\{w_n\}_{n=0}^{2}$ are non-negative real-valued constants adjusting the relative powers of the multiple scattering components. It is assumed that $\mathbb{E}\{r^2\} = 1$, so that $w_0^2 + w_1^2 + w_2^2 = 1$. These terms can be interpreted as the power weighting of a LOS component, a Rayleigh fading (first-order scattering) component, and a double Rayleigh fading (second-order scattering) component, respectively.

Double scattering has a special importance in physical geometry-based stochastic channel models [11], as it can result in severe degradation in symbol error probability and diversity gain [12]. In our case, double-Rayleigh fading may originate from second-order scatters, but it also describes the deep fades caused by occasional blocking and interaction from, e.g., bridges. The train carriage can be considered as electrically conducting planes, which lead to strong reflected and diffracted components. In addition, there is equipment for other systems located on the roof of Rx train, creating a complicated scattering propagation environment. Therefore, the train itself, together with scatters on both sides of slopes in cuttings and the occasional interaction by bridges and other "small" objects may result in fading that statistically can be described by double-Rayleigh fading phenomena.

To establish a model of the SSF for HSR cutting environments, we use the statistics of $r = |S_{SOSF}|$, which is characterized by its cumulative distribution function (CDF) as [9]

$$F_{SOSF}(r) = r \int_0^\infty e^{-w_1^2\kappa^2/4} \frac{4 J_1(r\kappa) J_0 w_0 \kappa}{4 + w_2^2 \kappa^2} d\kappa, \qquad (2)$$

where J_0 and J_1 are the Bessel functions of the first kind and zeroth and first-order, respectively. Following the definition in [12], the SOSF model can be specified by two parameters as follows

$$\beta = \frac{w_0^2}{w_0^2 + w_1^2 + w_2^2} \qquad \alpha = \frac{w_2^2}{w_0^2 + w_1^2 + w_2^2}, \qquad (3)$$

where $\alpha \geq 0$, $\beta \geq 0$, and $\alpha + \beta \leq 1$. A large α value indicates more severe fading conditions. Thus, we can define three special cases of the distribution of r in SOSF model: if $\alpha = 0, \beta > 0$, the SOSF distribution turns to a Ricean distribution; if $0 < \alpha < 1, \beta \approx 0$, the SOSF distribution simplifies to a Rayleigh and double-Rayleigh (RDR) distribution; a combination of Rice and double-Rayleigh (RiDR) is achieved when $0 < \alpha < 1, 0 < \beta < 1, \alpha + \beta < 1$. More importantly, we can easily calculate the Ricean K-factor with the parameter in the SOSF distribution as $K = \beta / 1 - \beta$, which is convenient when analyzing the statistics of the Ricean distribution.

IV. Experimental Characterization of Small-scale Fading Statistics in Cutting Scenarios

A. Parameter Estimation

The weighting factors (3) can be estimated based on a computationally simple method of moments [9]. The assumption

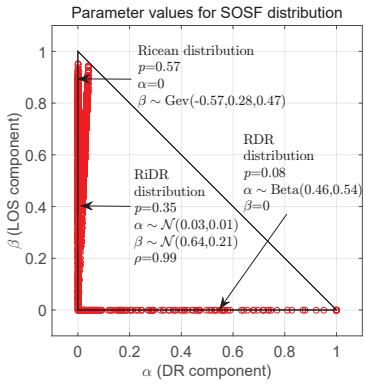

Fig. 2. Estimated parameters of the SOSF distribution.

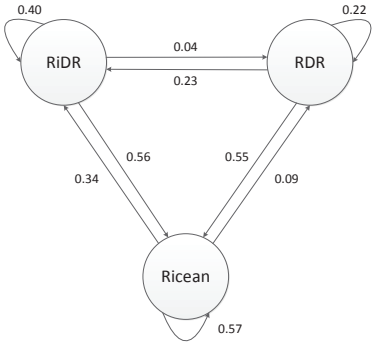

Fig. 3. State transition probabilities for the high speed rail cutting scenarios.

of this method is that there is no LOS component, therefore, by setting $w_0 = 0$ as the initial iteration parameter, the rest of the estimated weighting factors appear as

$$\widehat{w}_1^2 = M_2 - \widehat{w}_2^2, \tag{4}$$

$$\widehat{w}_2^2 = \sqrt{\frac{1}{2}M_4 - M_2^2}, \tag{5}$$

where M_k is the kth moment of SSF samples. The estimation process is then refined through an approximate maximum likelihood estimator. In this paper, we use the measurements No.1 to 5 to estimate the parameters (α, β) for the cutting scenario, and measurement No. 6 for a coarse validation.

B. Fading Distribution Analysis

The SOSF model can indicate the locations where deep fades occur. An example of the environment, distance-variant estimated factors (α, β), and Ricean K-factors in cutting No. 1 is given in Fig. 1. It can be concluded that the Ricean fading is the main fading distribution. Only scarcely, the double-Rayleigh fading components (red circles) are indicated when the Rx is passing below the crossing bridge (CBr 1-3). When the train is under the bridge, multipath propagation dominates and consequently it leads to a more severe fading in this region.

The Ricean K-factor is widespread for describing the small-scale fading characteristics. The K-factor in Fig. 1 also indicates the impact of bridges. Similarly, the results in [13] also verified that the K-factor shows a significant decline and then rises again when the train passes through cross-bridges. In fact, bridges have a non-negligible influence on propagation characteristics including extra propagation loss, LSF, and SSF. A more detailed analysis of propagation mechanism of bridges can be found in [14]. Since Ricean fading with LOS conditions, covers most small-scale fading behavior in the cutting scenario, it is necessary to investigate the statistics of the Ricean distribution. It is found that the K-factor can be modelled as an exponential function, when expressed in decibels. The median K-factor is found to be 2.1 dB, which is in agreement with the results in [7].

Estimated parameters of the SOSF model, constrained to a triangle of (α, β), are depicted in Fig. 2. We can see that all three different distributions derived from the SOSF distribution appear in this scenario. It is noted that the probability of LOS condition, which occurs for more than 90% (Ricean fading and RiDR fading) is dominant, as expected. In order to simulate the weighting factors, we parameterize (α, β) based on measurement data using a probabilistic approach. The distribution of the parameter (α, β) can be expressed as

$$\begin{aligned}(\alpha,\beta) \sim\ & 0.57\delta(\alpha)GEV(\beta|-0.57,0.28,0.47)\\ &+0.08\mathcal{B}(\alpha|0.44,0.53)\delta(\beta)\\ &+0.35\mathcal{N}_{\mu=[0.03,0.64],\sigma=[0.01,0.21],\rho=0.99}(\alpha,\beta),\end{aligned} \tag{6}$$

where δ is the Dirac delta function, *GEV* is a Generalized Extreme Value distribution, $\mathcal{B}$ is a Beta distribution, and $\mathcal{N}$ is a two-dimensional normal distribution with mean μ, standard deviation σ and correlation coefficient ρ.

C. Hidden Markov Model

In highly dynamic wireless scenarios it is important to describe the evolutional process of the SSF properly. A hidden Markov model (HMM), which can represent probability distributions over sequences of observations, is used to describe the transitions between different fading states [15]. Since the SSF behavior is modelled by a combination of three distributions, we use a three-state HMM to represent the transitions, as shown in Fig. 3, between (i) Ricean fading, (ii) RiDR fading and (iii) RDR fading. First, we estimate (α, β) within each local interval (20λ) of the measured SSF data, and then the fading state is determined according to the state definitions above. Finally, we estimate the transition probabilities between the states. The proportion of RiDR and RDR fading states are relatively high and these states frequently appear during the whole communication process. It can be concluded that Ricean fading is the primary propagation distribution but the deep fades, here represented by the double Rayleigh components, cannot be ignored in cutting propagation scenarios.

V. Model Implementation and Validation

To validate the proposed SOSF model for the SSF in cutting environments, we use the measurement data in cutting No. 6, whose results were not used in the parameter estimation of the above model. The generated SOSF amplitudes are compared with the measurement data and both first- and second-order statistics. The generation process is described as follows [16]

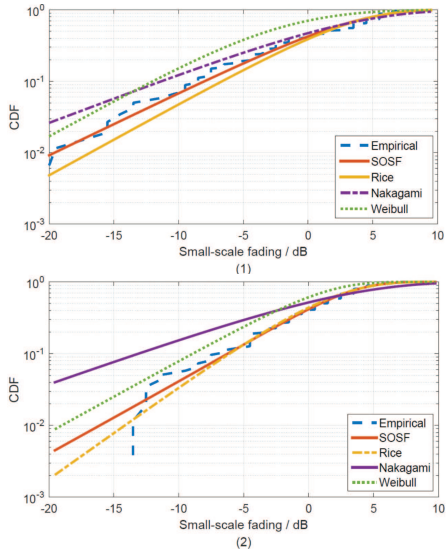

Fig. 4. Examples of CDF validation using the measurement data in rural cutting No. 6. (a) Deep fade window. (b) Typical window.

[17]: 1) Draw (α, β) according to the distribution described in Sec. IV with a random initial state of the HMM; 2) Generate a pre-defined number of complex fading realizations using equation (1); 3) For each iteration, new SOSF parameters (α, β) are generated if the state of the HMM changes, otherwise, the same SOSF parameters are used.

Fig. 4 presents two examples of alternative fading distributions for a deep fade window and a typical window. The non-parametric Kolmogorov-Smirnov (KS) test [18] is used to test the suitability of different fading distributions, rejection rates at a significance level of 0.05 are given in Table 2. The results demonstrate that the SOSF distribution provides a better fit to the empirical CDF than other alternatives. By analyzing the CDF for the SSF when the KS test suggests to reject the SOSF, it can be seen that in general this is due to even deeper fades in the empirical data compared to the analytical distribution. It is also worth mentioning that the validation with one additional cutting measurement data set may not be fully conclusive from a statistical perspective, but the feasibility of SOSF model in the cutting scenario can be verified.

VI. Conclusion

In this letter, we investigate multiple-scattering statistics of the SSF by using a peer-to-peer propagation model. A statistical analysis and characterization from the view of multi-scattering in cutting environments are presented. The SSF in cuttings can be described by the SOSF model, which can be treated as a combination of Ricean, Rayleigh fading and double Rayleigh fading. The transition between different fading states of the SOSF model is described by a HMM. It is found that the deep fades, here represented by the double Rayleigh components, cannot be neglected in HSR scenarios, the cross bridges along cuttings is the main reason for deep fades. Finally, the model is validated by measurement data conducted in another cutting. The results show that the SOSF distribution can be used to describe the SSF in HSR environments well. The main differences between SOSF distribution and other commonly used distributions are: i) the fading model is flexible and it can represent LOS plus multiple scatter components simply with two parameters, which allows adjustment of the severity of fading. ii) all parameters have clear physical meanings. iii) it is easily parameterized and can give a good approximation of the measured statistics especially at the deep fading zone in cutting scenarios.

TABLE II
KS tests of SSF in cutting No. 6, with significance level 0.05.

	SOSF	Rice	Nakagami	Weibull
Rejection rate	19.1%	26.7%	77.1%	98.1%

Acknowledgment

We thank Prof. C. Oestges at Université catholique de Louvain for providing code of SOSF parameter estimation.

References

[1] M. Yacoub, "Nakagami-m phase-envelope joint distribution: a new model," *IEEE Trans. Veh. Technol.*, vol. 59, no. 3, pp. 1552-1557, Mar. 2010.
[2] N. Beaulieu and S. Saberali, "A generalized diffuse scatter plus line-of-sight fading channel model," in *Proc. IEEE ICC*, Jun. 2014, pp. 5849-5853.
[3] B. Chen, Z. Zhong, B. Ai, and D. Michelson, "A geometry-based stochastic channel model for high-speed railway cutting scenarios," *IEEE Antennas Wireless Propag. Lett.*, vol. 14, pp. 851-854, Dec. 2014.
[4] T. Zhou, C. Tao, S. Salous, Z. Tan, L. Liu, and L. Tian, "Graph-based stochastic model for high-speed railway cutting scenarios," *IET Microw. Antennas Propag.*, vol. 9, no. 15, pp. 1691-1697, Oct. 2015.
[5] L. Tian, J. Zhang, and C. Pan, "Small scale fading characteristics of wideband radio channel in the U-shape cutting of high-speed railway," in *Proc. IEEE Veh. Technol. Conf.*, May 2013, pp. 1-5
[6] R. He, Z. Zhong, B. Ai, and J. Ding, "Propagation measurements and analysis for high-speed railway cutting scenario," *Electron. Lett.*, vol. 47, no. 21, pp. 1167-1168, Oct. 2011.
[7] R. He, Z. Zhong, B. Ai, J. Ding, Y. Yang, and A. F. Molisch, "Short-term fading behavior in high-speed railway cutting scenario: measurements, analysis, and statistical models," *IEEE Trans. Antennas Propag.*, vol. 61, no. 4, pp. 2209-2222, Apr. 2013.
[8] R. He, *et al.*, "High-speed railway communications: from GSM-R to LTE-R," *IEEE Veh Technol. Mag.*, vol. 11, no. 3, pp. 49-58, 2016.
[9] J. Salo, H. El-Sallabi, and P. Vainikainen, "Statistical analysis of the multiple scattering radio channel," *IEEE Trans. Antennas Propag.*, vol. 54, no. 11, pp. 3114-3124, Nov. 2006.
[10] B. Bandemer, C. Oestges, N. Czink, and A. Paulraj, "Physically motivated fast-fading model for indoor peer-to-peer channels," *Electron. Lett.*, vol. 45, no. 10, pp. 515-517, May 2009.
[11] A. F. Molisch, "A generic channel model for MIMO wireless propagation channels in macro- and microcells," *IEEE Trans. Signal Processing*, vol. 52, no. 1, pp. 61-71, Jan. 2004.
[12] J. Salo, H. EI-Sallabi, and P. Vainikainen, "Impact of double Rayleigh fading on system performance," in *Proc. Int. Symp. Wireless Pervasive Computing*, Jan. 2006, pp. 1-5.
[13] T. Zhou, C. Tao, L. Liu, and Z. Tan, "Ricean K-factor measurements and analysis for wideband radio channels in high-speed railway U-shape cutting scenarios," in *Proc. IEEE Veh. Technol. Conf.*, May 2014, pp. 1-5.
[14] K. Guan, Z. Zhong, B. Ai, and T. Kürner, "Propagation measurements and modeling of crossing bridges on high-speed railway," *IEEE Trans. Veh. Technol.*, vol. 63, no. 2, pp. 502-517, Feb. 2014.
[15] Y. Ephraim and N. Merhav, "Hidden Markov processes," *IEEE Trans. Inform. Theory*, vol. 48, no. 6, pp. 1518-1569, Jun. 2002.
[16] M. Gan, N. Czink, P. Castig, C. Oestges, F. Tufvesson, and T. Zemen, "Modeling time-variant fast fading statistics of mobile peer-to-peer radio channels," in *Proc. IEEE Veh. Technol. Conf.*, May 2011, pp. 1-5.
[17] E. Vinogradov, W. Joseph, and C. Oestges, "Measurement-based modeling of time-variant fading statistics in indoor peer-to-peer scenarios," *IEEE Trans. Antennas Propag.*, vol. 63, no. 5, pp. 2252-2263, May 2015.
[18] F. J. Massey, "The Kolmogorov-Smirnov Test for Goodness of Fit," *Journal of the American Statistical Association*, vol. 46, no. 253, 1951, pp. 68-78.